Theoretical analysis of nucleation and growth of ZnO nanostructures in Vapour Phase Transport growth

Journal:	*Crystal Growth & Design*
Manuscript ID:	cg-2011-00828y.R1
Manuscript Type:	Article
Date Submitted by the Author:	22-Aug-2011

Complete List of Authors:	Saunders, Ruth; Dublin City University, Dublin City University McGlynn, Enda; Dublin City University, School of Physical Sciences Henry, Martin; Dublin City University, School of Physical Sciences

Theoretical analysis of nucleation and growth of ZnO nanostructures in Vapour Phase Transport growth

Ruth B. Saunders,* Enda McGlynn, and Martin O. Henry

School of Physical Sciences, Dublin City University, Dublin, Ireland

E-mail: ruth.saunders3@mail.dcu.ie

Phone: +353 (1)700 5387. Fax: +353 (1)700 5384

Abstract

This paper discusses the growth atmosphere, condensing species and nucleation conditions relevant to vapour phase transport growth of ZnO nanostructures, including the molecular parameters and thermodynamics of the gas phase ZnO molecule and its importance compared to atomic Zn and molecular O_2. The partial pressure of molecular ZnO in a Zn/O_2 mix at normal ZnO growth temperatures is $\sim 6 \times 10^{-7}$ of the Zn partial pressures. In typical vapour phase transport growth conditions, using carbothermal reduction, the Zn vapour is always undersaturated while the ZnO vapour is always supersaturated. In the case of the ZnO vapour, our analysis suggests that the barrier to homogeneous nucleation (or heterogeneous nucleation at unseeded/uncatalysed areas of the substrates) is too large for nucleation of this species to take place, which is consistent with experimental evidence that nanostructures will not grow on unseeded areas of substrates. In the presence of suitable accommodation sites, due to ZnO seeds, growth can occur via Zn vapour condensation (followed by oxidation) and via direct condensation of molecular ZnO (whose flux at the surface, although less than that of Zn vapour, is still sufficient to yield an appreciable nanostructure deposit). The balance between these two

*To whom correspondence should be addressed

condensing species is likely to be a sensitive function of growth parameters and could explain both the diversity of reported nanostructure morphologies and the challenges to be faced in developing reproducible and scalable growth systems for specific applicable morphologies.

Introduction

ZnO nanostructures have a wide range of morphologies which are sensitive to growth parameters such as temperature, substrate type and the method used to generate source species.[1–5] Because of this sensitivity and morphological diversity, in order to reproducibly grow specific ZnO nanostructure morphologies, especially on an industrial scale, a greater theoretical understanding of the growth process is required. There is presently a scarcity of theoretical work on ZnO nanostructure growth, when compared to the number of observational reports of various ZnO morphologies.

One of the most widely used methods of growth is Vapour Phase Transport (VPT) with the Zn vapour generated by carbothermal reduction (CTR) of ZnO powder.[6] ZnO nanostructure growth via VPT involves four stages: generation of source species, transport of source species to the substrate, impingement of material onto the substrate (i.e condensation and nucleation) and incorporation of material into a nanostructure. This paper focuses on the production of the source species and the impingement of the material onto the substrate for ZnO nanostructure growth using Zn vapour generation via carbothermal reduction (CTR) of ZnO powders. We present a thermodynamic analysis of the gas atmosphere of the growth system and, based on this analysis a discussion of the likely condensing species for the case of a Si/SiO_2 substrate (a commonly used substrate material). We also discuss the saturation levels of ZnO vapour and nucleation conditions for molecular ZnO. We compare the theoretical results with experimental VPT growth results.

For the thermodynamic calculations in this paper we need parameters for the diatomic gaseous molecule ZnO, such as intermolecular distance r_e, the vibrational frequency ω_e, the dissociation

energy D_0, and the difference in energy between the first excited state and the energy of the ground state $\Delta\varepsilon$. Despite the relative dearth of experimental evidence for the existence and properties of this molecule, there are various reported values for these parameters. The molecular parameters of the ZnO(g) molecule were first studied by Brewer and Chandrasekharaiah[7] , whose technical report on gaseous monoxides estimated values of r_e and ω_e, respectively as 1.74 Å and 680 cm^{-1} (based on extrapolation from neighbouring species). These values have been refined over the years and compared with various theoretical measurements, and the current best estimates for r_e and ω_e are 1.72 Å and 780 cm^{-1} , respectively.[8] However, the value of the dissociation energy, D_0, has been continuously revised. Early reports (based on mass spectroscopy measurements) by Brewer and Mastick[9] and Anthrop and Searcy[10] gave upper limits (the experiments revealed no direct evidence of ZnO molecules) on D_0 of 3.99 eV and 2.86 eV, respectively. Later measurements, using guided ion-beam mass spectroscopy, have tended towards lower values of D_0 (1.61 eV[11]) which agree well with recent theoretical calculations of D_0 (e.g. 1.63 eV[12,13]). A value of 1.77 eV is used in the most recent version of the IVTANTHERMO database.[8] In our calculations we use four different parameter sets corresponding to the results of previous studies. These values are summarised in Table 1. In much of the subsequent analysis we show the data for sets 3 and 4 below, which represent the extreme values of D_0, and since D_0 tends to be a key parameter in determining the thermodynamic properties of the ZnO(g) molecule (as mentioned below also) and thus issues around nucleation and growth, the presentation of these data represent the range spanned by D_0 in sets 1-4.

Table 1: reported values for ZnO molecule

set	R_e(Å)	$\omega_e(cm^{-1})$	$D_0(eV)$	$\Delta\varepsilon(eV)$
Set1[12]	1.719	727	1.63	0.26
Set2[13]	1.719	770	1.63	0.305
Set3[11]	1.719	805	1.61	0.25
Set4[8]	1.72	780	1.77	0.32

Experimental

Growth substrates were prepared with ZnO seeds using a method combining drop coating and chemical bath deposition.[14] A small area of the sample was then dipped in H_2SO_4 and rinsed to remove the catalyst seeds and provide an unseeded area of the substrate for comparison. Non-metallic seeds were used, to eliminate the possibility of a vapour-liquid-solid (VLS) growth mode and ensure a vapour-solid (VS) growth mode. Equal amounts (0.06 g) of ZnO powder and graphite were mixed and placed in an alumina boat with the prepared seeded substrate placed face down above the mixed powders and placed in a furnace (see Figure 1). The furnace is flushed with Argon at 90 sccm for 50 minutes to remove residual oxygen, then heated to 1200 K with a mixed gas flow of 90 sccm of Argon and 4 sccm of Oxygen for 1 hour. The ZnO nanostructures were then examined using a scanning electron microscope (SEM, Karl-Zeiss EVO series). The pressure in the furnace is one atmosphere as the tube is open to the external atmosphere via the exhaust line.

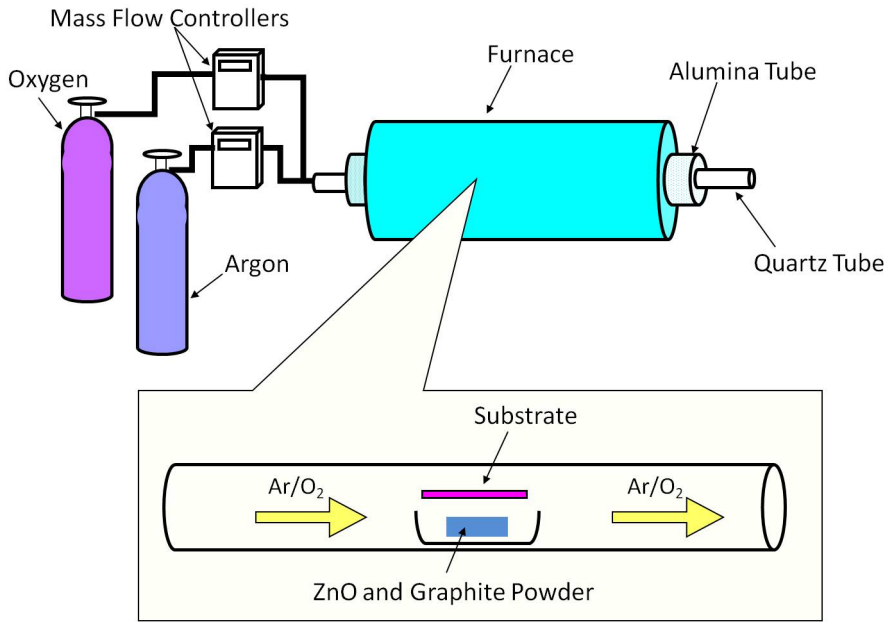

Figure 1: experimental set up

Thermodynamic Methods

Calculations of partial pressures of various components

In the first stage of VPT growth produces Zn vapour via the carbothermal reduction of ZnO powder. The Gibbs free energy of the carbothermal reduction reaction can be found using standard thermodynamic data (eg. from the IVANTHERMO[8] database). The reactions that describe CTR in the low ($T < 973K$) and high ($T > 973K$) temperature regime are:

$$\begin{aligned} T < 973K \quad & ZnO(s) + \tfrac{1}{2}C(s) \rightarrow Zn(g) + \tfrac{1}{2}CO_2(g) \\ T > 973K \quad & ZnO(s) + C(s) \rightarrow Zn(g) + CO(g) \end{aligned} \tag{1}$$

The equilibrium constant K_p of the carbothermal reduction reaction is calculated using the Gibbs free energy of the reaction, ΔG_r:

$$K_p = exp\left(\frac{-\Delta G_r}{RT}\right) \tag{2}$$

The partial pressure of Zn vapour is calculated using K_p as follows:

$$\begin{aligned} T < 973K \quad & K_p = \left(\frac{P_{Zn}}{P_{\ominus}}\right)\left(\frac{P_{CO_2}}{P_{\ominus}}\right)^{\frac{1}{2}} \\ T > 973K \quad & K_p = \left(\frac{P_{Zn}}{P_{\ominus}}\right)\left(\frac{P_{CO}}{P_{\ominus}}\right) \end{aligned} \tag{3}$$

where $P_{\ominus}$ is 1 bar. The partial pressure of Zn is normalized, so that the total partial pressure of all gases present (the sum of the partial pressures of the Ar, CO/CO_2,O_2 and Zn vapours) in the furnace tube remain at one atmosphere pressure, because the tube is open to the external atmosphere via the exhaust line. The vapour pressure of Zn was calculated using the Gibbs free energy of the

reaction $Zn(g) \rightarrow Zn(c)$ which gives the equilibrium pressure of Zn vapour over the most stable condensed Zn phase (Zn(c); solid below $\sim$ 692 K and liquid above). We have compared the results of our calculation of Zn vapour pressure with those of Rao[15] and find excellent agreement for the entire temperature range over which Rao presented data. The relative amounts of the ZnO gaseous species in the chamber are controlled by the Gibbs free energy of the reaction ΔG_r for the reaction $Zn(g) + \frac{1}{2}O_2(g) \rightarrow ZnO(g)$ where $\Delta G_r = G_{ZnO} - \frac{1}{2}G_{O_2} - G_{Zn}$. ΔG_r was calculated for ZnO, Zn and O_2, using a model of basic ideal monatomic and diatomic gases and the molecular parameters for ZnO(g) summarized in Table 1.

For diatomic ZnO and O_2:

$$G(T)_{ZnO,O_2} = RT \ln\left[\left(\frac{p\lambda_T^3}{k_bT}\right)\left(\frac{\theta_R\sigma}{T}\right)\left(1 - exp\left(-\frac{\theta_V}{T}\right)\right)\right] - RT \ln\left[\sum_i g_i exp\left(\frac{-\Delta\varepsilon_i}{(k_b)T}\right)\right] - D_0 \quad (4)$$

$$with \qquad \lambda_T = \hbar\left(\frac{2\pi}{k_bTm}\right) \qquad \theta_R = \frac{hcB}{k_b} \qquad B = \frac{\hbar}{4\pi cI} \qquad \theta_V = \frac{hc\nu_0}{k_b}$$

where I is the principal moment of inertia of the molecule, D_0 is the dissociation energy ,ω_e is the vibration frequency, r_e is the interatomic distance, $\Delta\varepsilon_i$ is the difference in energy between the i^{th} excited state and the energy of the ground state and g_i is the degeneracy of the excited electronic states. m is the molecular mass. R, c, h, $\hbar$, k_b have their usual meanings.[16]

For monatomic Zn(g):

$$G(T) = RT \ln\left[\frac{p\lambda_T^3}{k_bT}\right] \quad (5)$$

$$\text{with} \quad \lambda_T = \hbar \left(\frac{2\pi}{k_b T m} \right)$$

where m is the mass of atomic Zn. For the majority of our calculations we use the two extreme values of recently reported values of D_0 in Table 1 (1.61 eV and 1.77 eV, data sets 3 and 4, respectively in Table 1) to show the effects of changes in D_0. The equilibrium constant of the reaction $Zn(g) + \frac{1}{2}O_2(g) \rightarrow ZnO(g)$ was calculated using ΔG_r. The partial pressure of Zn vapour produced by CTR and the partial pressure of O_2 calculated from the relative value in the gas flow mix were used for the ZnO and O_2 values. The Zn vapour pressure is calculated using the reaction $Zn(g) \rightarrow Zn(c)$. Using the partial pressure of the Zn vapour from this reaction as the input to $Zn(g) + \frac{1}{2}O_2(g) \rightarrow ZnO(g)$ gives the vapour pressure of ZnO(g) over ZnO(s). We assume the reaction to create ZnO(g) has a negligible effect on the various other gas pressures, a fact borne out by the subsequent calculations.

Nucleation of ZnO crystals from ZnO molecular vapour

In the analysis of nucleation barriers we assume that the nucleating crystal is a hexagonal cross section cylinder, which is consistent with most of experimental reports. We use the Gibbs-Curie-Wulff theorem to find the equilibrium shapes of both homogeneously and heterogeneously nucleated crystals, following the treatment outlined by Markov.[17] ZnO is an anisotropic material and thus has different values of surface energy for different faces. Recent data indicates that for the prismatic plane surface (1010) the surface energy is $\sigma_p = 1.15\ \mathrm{J/m^2}$ and for the basal plane surface (0001) it is $\sigma_b = 2.0\ \mathrm{J/m^2}$.[18]

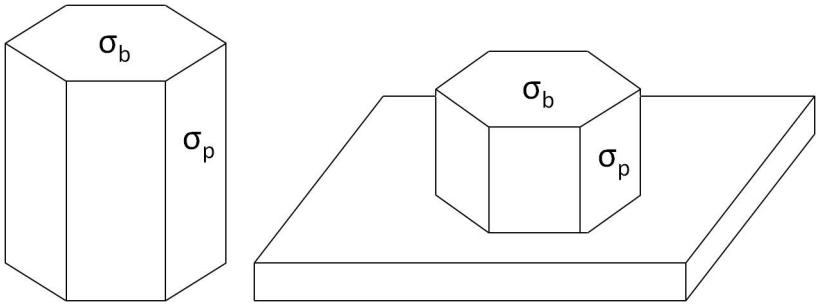

Figure 2: (a) homogeneously nucleating crystal and (b) heterogeneously nucleating crystal

The energy barrier to homogeneous nucleation is found by simple geometry and is given by:

$$\Delta E_{\text{hom}} = \frac{16\sqrt{3}{v_m}^2{\sigma_p}^2\sigma_b}{(RT\ln[s+1])^2} \tag{6}$$

where s is the degree of supersaturation, σ_b is the basal plane energy and σ_p is the prismatic plane energy, v_m is the molar volume of ZnO $\left(v_m = 14.52\times10^{-16}\ \text{m}^3/\text{mole}^{19}\right)$. At a temperature of 1200 K the energy barrier to homogeneous nucleation is 2.65 eV, more than 200 times the thermal energy at this temperature. The classical homogeneous nucleation rate $\text{I}_{\text{hom}}\left(\text{events}/\text{m}^3\text{s}\right)$ for hexagonal particles is calculated following the procedure described by Markov[17] where p is the partial pressure of the molecular ZnO vapour:

$$I_{\text{hom}} = \left(\frac{p^2}{k_b^2T^2\rho}\right)\left(\frac{2m}{\sqrt{3}\pi^2}\right)^{\frac{1}{2}}\left(3+\frac{6\sigma_b}{\sigma_p}\right)\left(\frac{\sigma_p}{\sqrt{\sigma}_b}\right)exp\left(-\frac{\Delta E_{\text{hom}}}{k_bT}\right) \tag{7}$$

We have again used the Gibbs-Curie-Wulff theorem to find the equilibrium shape of the nucleating particle using the surface energies of ZnO as inputs to determine the aspect ratios of the hexagonal cylinder. To calculate the energy barrier for heterogeneously nucleating particles we followed the method of treatment outlined by Markov. The contact angle for the ZnO on the substrate is taken as $\theta = 90^\circ$ consistent with experimental data and growth on non-wetting substrates.

An additional term to accounts for the strain due to the lattice mismatch between the substrate and ZnO.[20] The analysis predicts an energy barrier ΔE_{het} to heterogeneous 3D nucleation for such a nucleus of:

$$\Delta E_{\text{het}} = 8\sqrt{3}\sigma_p{}^2\sigma_b\left(\frac{2\nu_m}{2RT\ln[s+1]-\nu_m Y\varepsilon^2}\right)^2 \tag{8}$$

where Y is the Young's modulus of ZnO (estimated to be 100 GPa[21]), N_0[17] is the number of adsorption sites (1×10^{15} cm^{-2}), and ε is the lattice mismatch between ZnO and the silicon substrate $\left(\varepsilon=\frac{a_{Si}-a_{ZnO}}{a_{Si}}=0.4\right)$. In reality, the lattice mismatch ε would be larger than the value 0.4 calculated using the lattice parameters of Si, because the substrate will be silicon with a thin layer of silicon dioxide. The lattice mismatch between ZnO and SiO_2 will be ~ 1.4.[22–24] This would lead to a much greater energy barrier. We take the calculation for Si as a maximum number of nucleation events, but in an experimental situation the number would be smaller, due to the presence of the layer of SiO_2. This gives an energy barrier to heterogeneous nucleation of 8.63 eV at a temperature of 1200 K. The nucleation rate for heterogeneously nucleating particles is found to be:

$$I_{\text{het}} = \frac{\nu_m N_o}{N_A\sqrt{\sigma_b\sqrt{3}}}\left(\frac{p}{\pi m k_b T}\right)\left(\frac{2RT\ln[s+1]-\nu_m Y\varepsilon^2}{2\nu_m}\right)\frac{4\lambda_d{}^2}{a_d}exp\left(-\frac{\Delta E_{het}}{k_b T}\right) \tag{9}$$

where λ_d is the estimated diffusion length of ZnO on silicon (here estimated to be 1 μm based here estimated to be 1 micron based on species diffusion lengths deduced for nanowire growth in other binary compound materials at about 1200 K[25]). The hopping distance is approximated as $a_d = 0.3\ nm$.[26]

Results

Figure 3 shows the Gibbs free energy of reaction ΔG_r for each parameter set as a function of temperature over the temperature range of interest for VPT, from 300 K to 2000 K. The values for the Gibbs free energy of reaction vary for each set. The variation of interatomic distance, frequency

and electronic energy level separation from set to set appear to have little impact on ΔG_r and the differences between the ΔG_r values of each set depend mainly on the dissociation energy of that set. The Gibbs free energy of reaction for the generation of ZnO is positive for each set despite the difference in absolute values, giving a very small equilibrium constant and consequently a small partial pressure of ZnO(g) in all cases.

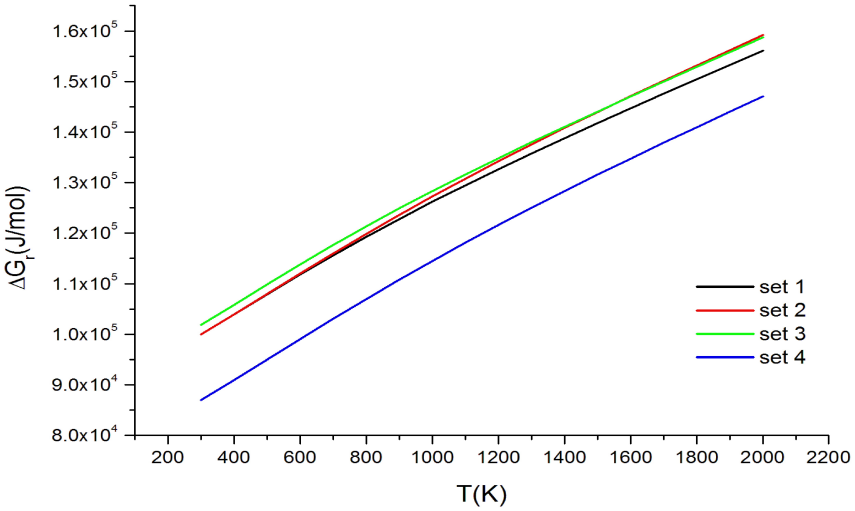

Figure 3: ΔG_r for reaction $Zn(g) + \frac{1}{2}O_2(g) \rightarrow ZnO(g)$

The calculated partial pressures and vapour pressures of Zn and ZnO are shown in Figure 4(a) and Figure 4(b) as a function of temperature over the temperature range of interest for VPT. The partial pressure of Zn, at the growth temp of 1200 K, is 0.294 atm compared to a partial pressure of ZnO of 1.73×10^{-7} atm. This means that the partial pressure of ZnO vapour is $\sim 6 \times 10^{-7}$ smaller than the partial pressure of the Zn vapour, a very substantial difference.

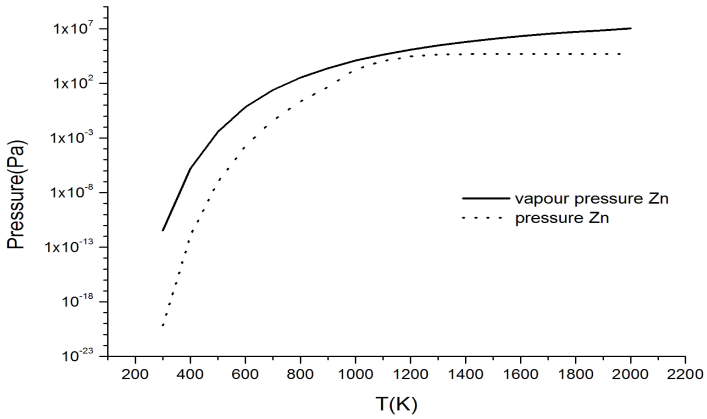

(a)

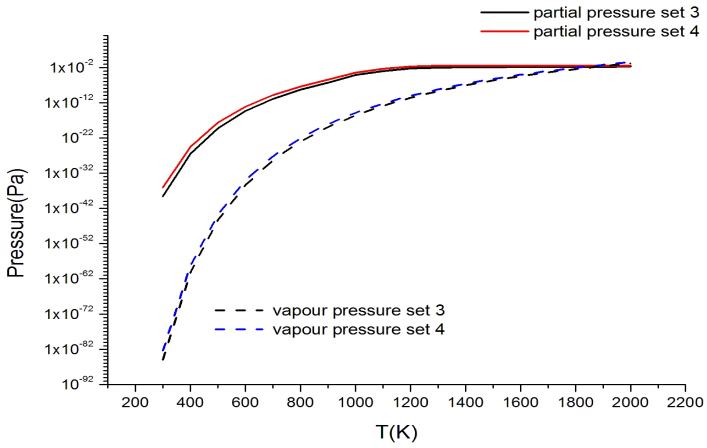

(b)

Figure 4: Partial and vapour pressures of (a) Zn (b) ZnO

The degree of saturation of a vapour is given by $s = \frac{p - p_0}{p_0}$ where p_0 is the vapour pressure. The degree of supersaturation indicates whether a vapour is undersaturated (s $<$1) or supersaturated (s $>$1), and determines the likelyhood of a molecule which has condensed onto the surface remaining on the surface and ultimately incorporating into a growing crystallite or evaporating back to the vapour state. Figure 5(a) shows the degree of saturation of Zn vapour over the most stable condensed Zn phase, Zn(c), while Figure 5(b) shows the saturation of ZnO vapour over solid ZnO for two values of molecular parameters (sets 3 and 4 from Table 1). Figure 5(c) is the saturation of Zn vapour over solid ZnO (i.e the saturation of Zn over an already growing nanowire

crystal).

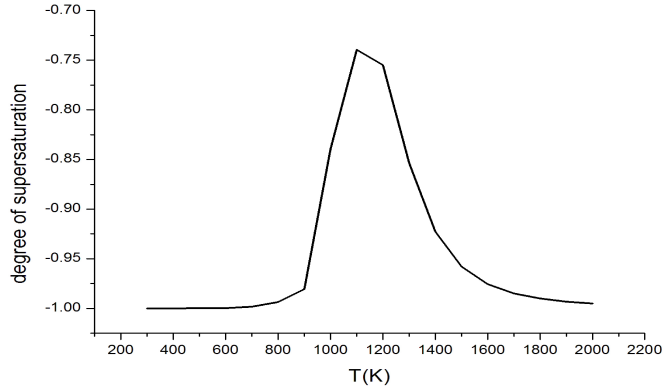

(a)

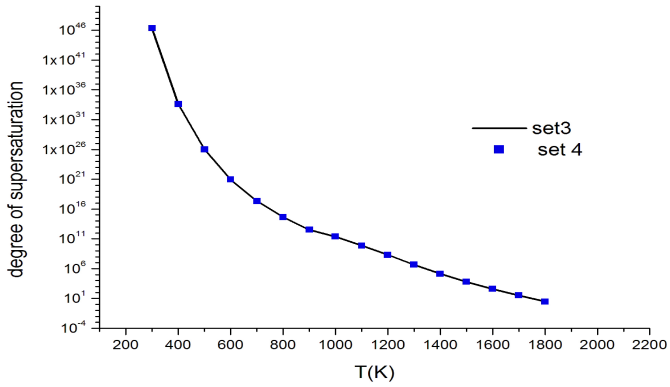

(b)

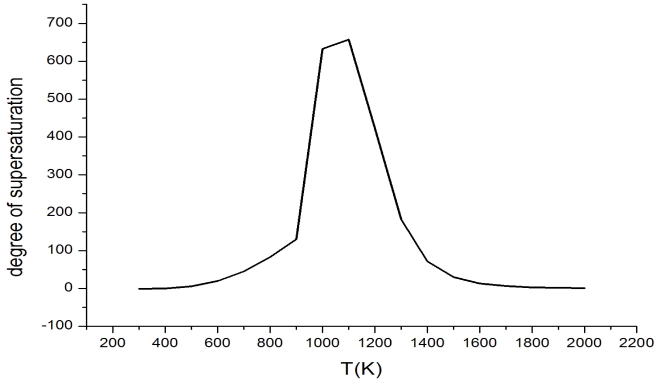

(c)

Figure 5: Degree of saturation for (a) Zn(g) over Zn(c), (b) ZnO(g) over solid ZnO for two values of molecular parameters (sets 3 and 4 from Table 1) and (c) Zn(g) over solid ZnO

The Zn vapour is undersaturated at all temperatures. A negative value for the degree of saturation would indicate that the number of molecules leaving the surface is greater than the number arriving at the surface. However the Zn vapour over solid ZnO is supersaturated at all temperatures. The pressure of ZnO is far, far greater than the vapour pressure of ZnO, showing that ZnO(g) is supersaturated at all temperatures to a large degree.

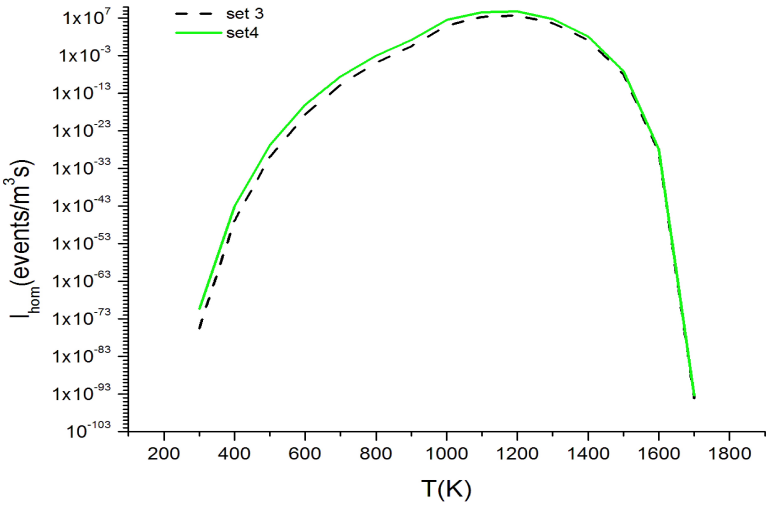

(a)

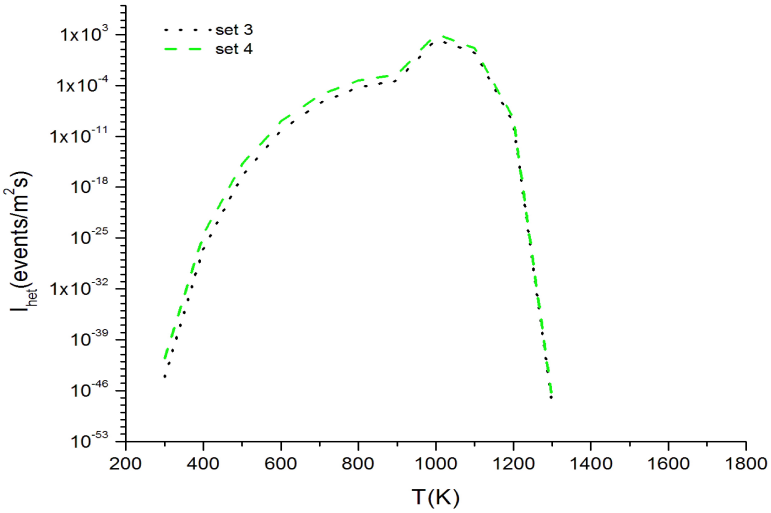

(b)

Figure 6: Rate of nucleation for (a) homogeneous nucleation and (b) heterogeneous nucleation

Figure 6(a) and Figure 6(b) show the rate of nucleation for homogeneous and heterogeneous growths are shown in for two values of molecular parameters (sets 3 and 4 from Table 1). At a growth temperature of 1200K, the rate of homogeneous nucleation (rate of nucleation events per unit volume) $I_{\text{hom}} = 6.58 \times 10^8$ events$/m^3 s$ and the rate of heterogeneous nucleation (rate of nu-

cleation events per surface area) $I_{\text{het}} = 2.57 \times 10^{-9}$ events$/m^2 s$.

The results of the VPT ZnO nanowire growth on Si substrates with a native oxide are shown in Figure 7. The SEM image shows well aligned ZnO nanowires of length $\sim 2\ \mu m$ and of diameter ~ 75 nm on seeded areas of the substrate. There are no nanowires on the bare/unseeded area of the substrate.

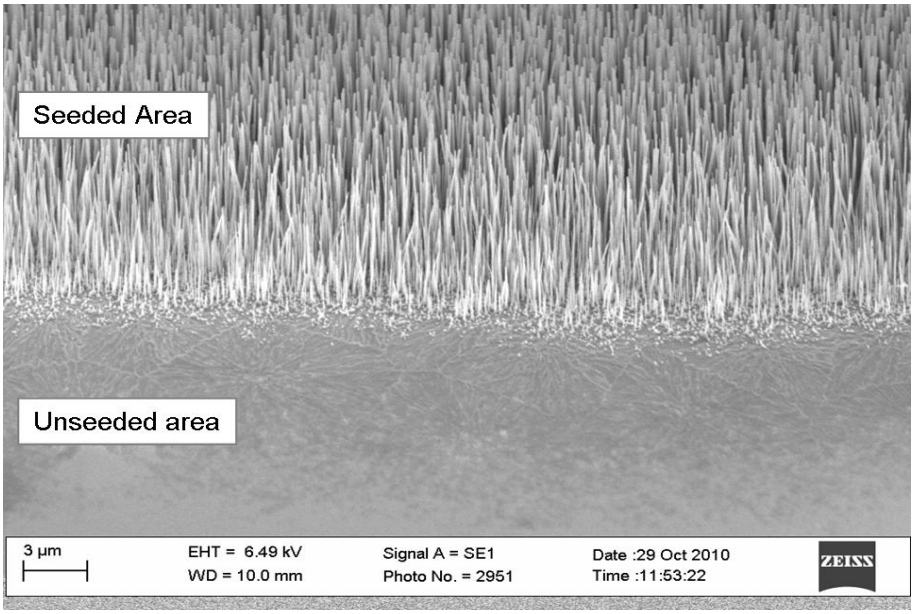

Figure 7: Nanowire growth on bare/unseeded and seeded areas of the silicon substrate

Discussion

Calculation of the partial pressures and degree of saturation of Zn vapour over Zn(c) show that while the partial pressure of Zn vapour is relatively large, the vapour is undersaturated and so will not condense on the surface unless energetically suitable accommodation sites exist. Note however that the saturation of Zn vapour over solid ZnO is 422, at a growth temperature of 1200 K (and significantly greater than 1 over a wider temperature range from 600 K to 1600 K), which means that once the nanostructure has nucleated and started to grow, Zn vapour molecules will readily condense at the ZnO crystallite, and react with O_2 to form ZnO. Conversely, the partial pressure of

ZnO is very small, but the vapour present is significantly supersaturated, meaning it would be expected to condense readily either in the gas phase or on the surface, if it can overcome the relevant nucleation barrier. Because we experimentally observe no nanostructure growth without suitable accommodation sites (seeds) for growth, on Si substrates at a temperature of $\sim$ 1200 K, we expect that barriers to nucleation will probably play an important role along with other effects.

The rate of homogeneous nucleation at 1200 K is $I_{\mathrm{hom}} = 6.58 \times 10^{8}$ events$/m^3 s$. In a volume of $1\ cm \times 1\ \mu m \times 1\ \mu m$ (a surface area of $1\ \mu m^2$ and a distance of $1\ cm$ between source and substrate), over a growth time of 1 hour, the number of nucleation events is 0.0236. This is consistent with experimental results showing little or no nucleation of nanostructures on bare substrates. While this nucleation rate is small, it is conceivable that occasional nuclei might form homogeneously and land on the substrate surface, for example we note that occasionally ZnO nanostructures are seen on unseeded areas of substrate. We also note that during growth, the native silicon dioxide tends to grow around and consume surface particulates, which also will mitigate against substantial ZnO growth on these nuclei.[27]

The energy barrier to heterogeneous nucleation at 1200 K is 8.63 eV. This is a large value compared to the thermal energy at this temperature due to the large lattice mismatch between the ZnO and Si/SiO_2 substrate, which leads to a large strain term in the energy barrier to nuclei formation. The rate of heterogeneous nucleation for ZnO on a Si/SiO_2 substrate at 1200 K is $I_{\mathrm{het}} = 2.57 \times 10^{-9}$ events$/m^2 s$. In an area of $1\ \mu m \times 1\ \mu m$, over a growth time of 1 hour, the number of events is 9.25×10^{-18}. This is a negligible number of nucleation events and is consistent with the experimental results, showing no growth on such an unseeded Si/SiO_2 substrate, at such temperatures as shown in Figure 7. The ZnO vapour, despite being strongly supersaturated, is unlikely to nucleate on bare substrates due to the energy barriers to homogeneous and heterogeneous nucleation. Thus neither Zn vapour nor ZnO vapour is likely to condense and nucleate ZnO crystals on bare silicon substrates.

We now consider the case where suitable accommodation sites or 'seeds' nanostructure growth will take place. In order to determine whether growth takes place via condensation of Zn vapour (followed by oxidation) or direct condensation of ZnO vapour the impingement rate of the molecules was calculated using the Knudsen relation

$$J = \frac{p}{\sqrt{2\pi m k_b T}} \tag{10}$$

Using the partial pressures for Zn, ZnO and O_2 the impingement rate was calculated. The sticking coefficients α_{Zn} and α_{ZnO} for Zn and ZnO are assumed to be unity. The sticking coefficient for oxygen is not unity as it is a diatomic molecule and the dissociation of oxygen molecules to react with Zn atoms is a complex process. The sticking coefficient $\alpha_{\mathrm{O_2}}$ was found using an expression derived by Carlos Rojo et al.[28]

$$\alpha_{O_2} = 0.27966 \exp\left[\frac{-14,107.9578}{T}\right] \tag{11}$$

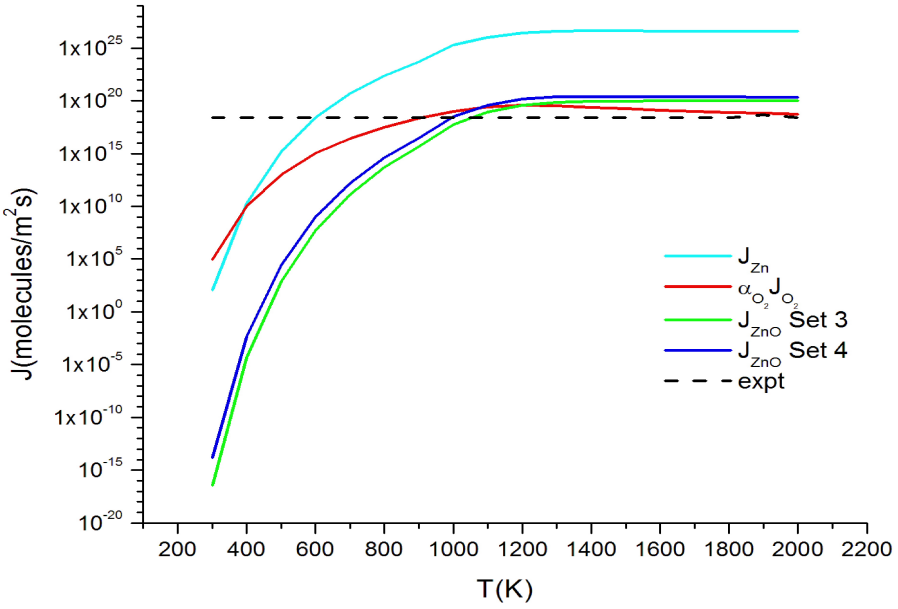

Figure 8: Effective impingement rates for Zn, O_2 and ZnO

In order to be compatible with the experimental results in figure 7 the impingement rate required for the experimentally observed nanowire growth is estimated assuming an average density of 25 nanorods/μm^2 of length 2 μm and diameter 75 nm over a growth time of 1 hour. The estimated impingement rate is 2.4×10^{18} molecules/m^2s. The impingement of Zn molecules is the highest, however it will be limited by the amount of O_2 arriving at the surface, in order for the Zn molecules to be oxidized to form ZnO and thus determined by $\alpha_{O_2} J_{O_2}$. The impingement rate of ZnO molecules, while smaller than Zn, is still more than required for the growth observed at temperatures greater than 1000 K. Clearly the gas pressures, nucleation and growth rates resulting from our earlier analyses are upper bounds. Kinetic aspects of the CTR reaction, the reaction of Zn vapour and O_2 to form ZnO vapour and the vapour transport from source to substrate is likely to lead to smaller values for all of these quantities, compared to the thermodynamic analysis, which explains the lower actual growth rates. Nevertheless, good order of magnitude agreement is found between theory and experiment. This indicates that both species can contribute to the growth of

ZnO nanowires in VPT growth via CTR. We suggest that the diversity of ZnO nanostructure morphologies observed experimentally is related to the simultaneous presence of these two growth channels and their varying relative importance in different growth conditions, which will depend on, inter alia, the varying temperature dependences and time-scales of surface diffusion of Zn and ZnO species and the oxidative reaction and incorporation of Zn atoms into the growing ZnO nanocrystals. This balance is likely to be a sensitive function of growth parameters, thus explaining both the diverse nanostructure morphologies reported and the challenges faced in developing reproducible and scalable growth systems for specific applicable morphologies. Various authors have suggested that ZnO growth proceeds by (a) Zn(g) condensation followed by oxidation,[29] (b) ZnO(g) condensation into crystalline ZnO,[30] or (c) by a combination of such processes, with the dominant one being dependent on experimental conditions.[31] Our data support the final hypothesis, and the key aspect of our findings is that the simultaneous presence of these two growth channels, over a range of growth temperatures, and their varying relative importance at different growth conditions, produce the diversity of ZnO nanostructure morphologies observed experimentally.

Conclusions

This paper reports theoretical data concerning the thermodynamic conditions in the growth atmosphere for CTR-VPT growth of ZnO nanowires. We show that in typical carbothermal vapour phase transport growth conditions the Zn vapour is always undersaturated while the ZnO vapour is always supersaturated, although the absolute pressure of the ZnO(g) species is $\sim 6 \times 10^{-7}$ less than that of the Zn(g) species. Based on these results, we discuss the potential condensing/nucleating species. The undersaturated Zn(g) species will nucleate only at locations with energetically suitable accommodation sites which is consistent with experimental data. Despite its low absolute pressure, the ZnO(g) flux cannot be neglected as a potential source of nanowire growth. However, in the case of this species, an analysis based on classical nucleation theory suggests that the nucleation barrier is such that homogeneous nucleation (and also heterogeneous nucleation on the

commonly used inert substrates, such as Si/SiO_2 in the absence of either metal catalysts or ZnO buffer layers) is not possible. Thus our conclusions agree with the experimental evidence that ZnO nanostructure growth using CTR-VPT requires metal catalysts or pre-deposited ZnO nucleation points. In the presence of suitable accommodation sites, due either to metal catalysts or predeposited ZnO seeds, growth can occur via Zn vapour condensation (followed by oxidation) and also via direct condensation of molecular ZnO (whose flux at the surface, although less than that of Zn vapour, is still sufficient to yield an appreciable nanostructure deposit). The presence of two growth channels and the balance between them offers a possible explanation for the diverse morphologies observed in ZnO nanostructure growth.

This discussion of CTR-VPT growth may also be relevant to other gas phase growth techniques, where Zn(g) vapour and oxygen are the main growth species, such as thermal or electron beam evaporation of ZnO / Zn powders in various oxygen-containing atmospheres, where similar conclusions concerning the growth mechanism may apply. However, techniques such as PLD, which involve a range of particulate sizes and charge states, or MOCVD, where the chemistry and reactions of the various gaseous species are substantially different to the present case, will undoubtedly require a more complex analysis, taking into account the specific features of these techniques. This will also certainly be the case for chemical solution techniques.

We believe that the results presented above provide a general framework from which to view ZnO nanowire growth processes of the VPT type. Physical insights gained from this thermodynamic analysis approach to understand the relatively narrow range of growth processes of the VPT type may ultimately be applicable to a broader range of ZnO nanostructure growth processes and may lead to more general understanding of the key aspects which determine the morphology of this nanomaterial.

Acknowledgements

RBS acknowledges the award of an Irish Research Council for Science, Engineering and Technology (IRCSET) Embark Postgraduate Research Scholarship. EMCG acknowledges financial support from a range of grant funding sources including SFI PI and RFP grant sources, which have enabled the development of the experimental infrastructure used in this work over a number of years . We also acknowledge financial support from the School of Physical Sciences, Dublin City University (DCU) and infrastructural support from the National Centre for Plasma Science and Technology (NCPST) at DCU. RBS gratefully acknowledges helpful discussions with Dr. Jonas Johansson (Lund University, Sweden) on a number of issues discussed in this work. RBS also gratefully acknowledges the assistance of Mr. Seamus Garry with SEM image acquisitions.

References

[1] Wang, Z. *JOURNAL OF PHYSICS-CONDENSED MATTER* **2004**, *16*, R829–R858.

[2] Grabowska, J.; Meaney, A.; Nanda, K.; Mosnier, J.; Henry, M.; Duclere, J.; McGlynn, E. *PHYSICAL REVIEW B* **2005**, *71*.

[3] Wang, J.; Zhuang, H.; Li, J.; Xu, P. *APPLIED SURFACE SCIENCE* **2011**, *257*, 2097–2101.

[4] Wongchoosuk, C.; Subannajui, K.; Menzel, A.; Burshtein, I. A.; Tamir, S.; Lifshitz, Y.; Zacharias, M. *JOURNAL OF PHYSICAL CHEMISTRY C* **2011**, *115*, 757–761.

[5] Kumar, R. T. R.; McGlynn, E.; Biswas, M.; Saunders, R.; Trolliard, G.; Soulestin, B.; Duclere, J. R.; Mosnier, J. P.; Henry, M. O. *JOURNAL OF APPLIED PHYSICS* **2008**, *104*.

[6] Biswas, M.; McGlynn, E.; Henry, M. O.; McCann, M.; Rafferty, A. *JOURNAL OF APPLIED PHYSICS* **2009**, *105*.

[7] Brewer, M., L.; Chandrasekharaiah *Lawrence Berkeley Radiation Laboratory Report* **1960**,

[8] values used in IVANTHERMO database by Glushko Thermocenter of the Russian Academy of Sciences listed at http://www.chem.msu.su/rus/tsiv/Zn/table.Zn.6.html,.

[9] Brewer, D., L.; Mastick *J. Chem. Phys.* **1951**, *19*, 834.

[10] ANTHROP, D.; SEARCY, A. *JOURNAL OF PHYSICAL CHEMISTRY* **1964**, *68*, 2335–&.

[11] Fancher, C.; de Clercq, H.; Thomas, O.; Robinson, D.; Bowen, K. *JOURNAL OF CHEMICAL PHYSICS* **1998**, *109*, 8426–8429.

[12] Bauschlicher, C.; Partridge, H. *JOURNAL OF CHEMICAL PHYSICS* **1998**, *109*, 8430–8434.

[13] Kim, J.; Li, X.; Wang, L.; de Clercq, H.; Fancher, C.; Thomas, O.; Bowen, K. *JOURNAL OF PHYSICAL CHEMISTRY A* **2001**, *105*, 5709–5718.

[14] Byrne, D.; McGlynn, E.; Kumar, K.; Biswas, M.; Henry, M. O.; Hughes, G. *CRYSTAL GROWTH & DESIGN* **2010**, *10*, 2400–2408.

[15] Rao, Y. *Stoichiometry and thermodynamics of metallurgical processes*; Cambridge University Press: Cambridge, U.K., 1985.

[16] Chase, M., Ed. *NIST-JANAF Thermochemical Tables, 4th ed*; AmericanChemical Society, American Institute of Physics for the National Institute of Standards and Technology, Woodbury, N.Y., 1998.

[17] Markov, I. *Crystal Growth for Beginners, 2nd edition*; World Scientific, London, 2003.

[18] Wander, A.; Schedin, F.; Steadman, P.; Norris, A.; McGrath, R.; Turner, T. S.; Thornton, G.; Harrison, N. M. *Phys. Rev. Lett.* **2001**, *86*, 3811–3814.

[19] Lide, D., Ed. *CRC Handbook of Chemistry and Physics, 73rd Edition*; CRC Press, 1992.

[20] Wessels, B. *JOURNAL OF VACUUM SCIENCE & TECHNOLOGY B* **1997**, *15*, 1056–1058.

[21] Stan, G.; Ciobanu, C. V.; Parthangal, P. M.; Cook, R. F. *NANO LETTERS* **2007**, *7*, 3691–3697.

[22] Won Mook Choi, D. C. K. K. H.-J. S. S.-M. Y. J.-Y. C. S.-W. K., Kyung-Sik Shin *Nano Research* **2011**, *4(5)*, 440–447.

[23] Ng, K.; Vanderbilt, D. *PHYSICAL REVIEW B* **1999**, *59*, 10132–10137.

[24] Shi, N.; Ramprasad, R. *PHYSICAL REVIEW B* **2006**, *74*.

[25] Dayeh, S. A.; Yu, E. T.; Wang, D. *NANO LETTERS* **2009**, *9*, 1967–1972.

[26] Smith, D. L. *Thin-Film Dep, Principle and Practice*; McGraw-Hill, 1995.

[27] Daragh Byrne-private communication.

[28] Rojo, J. C.; Liang, S.; Chen, H.; Dudley, M. Physical vapor transport crystal growth of ZnO. 2006.

[29] Borchers, C.; Muller, S.; Stichtenoth, D.; Schwen, D.; Ronning, C. *JOURNAL OF PHYSICAL CHEMISTRY B* **2006**, *110*, 1656–1660.

[30] Kubo, M.; Oumi, Y.; Takaba, H.; Chatterjee, A.; Miyamoto, A.; Kawasaki, M.; Yoshimoto, M.; Koinuma, H. *PHYSICAL REVIEW B* **2000**, *61*, 16187–16192.

[31] Im, S.; Jin, B.; Yi, S. *JOURNAL OF APPLIED PHYSICS* **2000**, *87*, 4558–4561.

For Table of contents use only

Theoretical analysis of nucleation and growth of ZnO nanostructures in Vapour Phase Transport growth

Ruth B. Saunders, Enda McGlynn, Martin O. Henry

This paper discusses the growth atmosphere, condensing species and nucleation conditions relevant to vapour phase transport growth of ZnO nanostructures, including the molecular parameters and thermodynamics of the gas phase ZnO molecule and its importance compared to atomic Zn and molecular O_2.

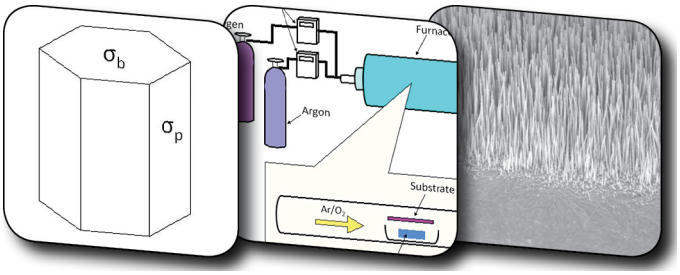

Figure 9: Table of contents graphic